Broadband spectrum generation with compact Yb-doped fiber laser by intra-cavity cascaded Raman scattering

Zikai Dong (董自凯), Yanrong Song (宋晏蓉)*, Runqin Xu (徐润亲), Yu Zheng (郑 煜), Jinrong Tian (田金荣), and Kexuan Li (李克轩)

College of Applied Sciences, Beijing University of Technology, Beijing, 100124, PR China
**Corresponding author: yrsong@bjut.edu.cn*

Received December 1, 2016; accepted April 14, 2017; posted online May 10, 2017

We experimentally demonstrate a cascaded Raman scattering continuum, utilizing a compact mode-locked Yb-doped fiber laser based on a nonlinear polarization rotation technique in the all normal dispersion regime. There is no physical filter or polarization controller in the oscillator, and a different mode-locked operation is achieved, corresponding to the extra fiber location in the oscillator. The broadband spectrum generation owes to the enhanced stimulated Raman scattering progress. The maximum output average power and peak power are 14.75 nJ and 18.0 W, and the short coherence light is suited for optical coherence tomography.

OCIS codes: 140.3510, 140.3550, 140.4050, 070.4340.
doi: 10.3788/COL201715.071408.

The nonlinear polarization rotation (NPR) technique has become one of the main techniques to achieve mode-locked fiber lasers for its compactness, implementation, and low cost[1]. NPR mode-locked fiber lasers operating in the all normal dispersion (ANDi) regime[2] have been widely investigated for their high pulse energy[3–6]. Typical ANDi mode-locked fiber lasers include a spectral filter and a polarization controller, which play crucial roles to balance intra-cavity dispersion and nonlinear effects[7]. Chirped pulses are generated with the interaction between nonlinear phase accumulation and spectral filtering in the ANDi regime[8]. References [9,10] revealed that a physical intra-cavity bandpass filter was not crucial for the generation of the chirped pulses. Reference [11] reported that a self-pulse was generated without polarization controlling devices, and the fiber laser utilized the active fiber reabsorption effect as a saturable absorber for mode locking. Moreover, a self-started unidirectional dissipative soliton (DS) was generated in Yb-doped fiber (YDF) lasers without an isolator based on the NPR technique due to the cavity directional nonlinearity asymmetry[12]. The above results show the possibility to realize a more compact and low-cost fiber laser by utilizing a simplified NPR technology.

Broadband spectrum generation at 1.0–1.2 μm has gained much attention for applications in gas sensing, optical communication systems, and wavelength tunable and optical coherence tomography (OCT). An alternative way to generate a broadband spectrum is by using noise-like pulse (NLP) emission in an optical fiber ring cavity. Reference [13] reported that the NLP with a spectrum bandwidth of up to 131 nm (FWHM) was obtained in a YDF laser. Raman scattering generated broadband spectrum in optical fiber lasers has also been widely investigated[14–17]. In most experiments, multi-order Raman scattering generation is realized in an extra-cavity configuration, in which a long fiber is used to reduce the pump power threshold of stimulated Raman scattering (SRS)[18,19] and provide enough gain for cascaded SRS generation[20–23]. In recent years, photonic crystal fibers (PCFs) are also utilized for higher nonlinear gain[24–27]. However, the extra-cavity configuration needs high peak power or high pulse energy to pump the fiber. Because the peak power and pulse energy inside the laser cavity are high, the intra-cavity configuration for multi-order Raman scattering generation is simpler[23].

In this Letter, there are no physical filters and polarization controllers in the laser cavity. A mode-locked pulse train is achieved in the ANDi regime based on the NPR technique. The fiber birefringence-induced filtering effect (FBFE) is the main reason for mode locking in our laser setup. The extra 20 m long single mode fiber (SMF) is inserted in two different positions, where the DS operation and NLP operation are achieved correspondingly. The nonlinear effect is obviously enhanced in the NLP regime, and broadband spectrum generation is owed to the enhanced SRS progress. The maximum output average power and peak power are 14.75 nJ and 18.0 W, so the laser is an ideal source for OCT.

The experimental setup of a simplified Yb-doped mode-locked fiber laser is shown in Fig. 1. There is no physical filter and polarization controller in it. The pump source is a 976 nm single mode laser diode (LD) with the maximum output power of 600 mW, which core-pumped the gain fiber through a filter wavelength division multiplexer (FWDM) with a central wavelength of 1030 nm. The polarization-independent isolator (PI-ISO) is inserted to force the laser to operate unidirectionally. The gain fiber is a 23 cm long YDF with the absorption coefficient of 1200 dB/m at 976 nm. A length of 24.5 m passive SMF is used to increase the nonlinear effect and induce a large dispersion. The polarization beam splitter (PBS) converts NPR into amplitude modulation and serves as the output coupler to couple the portion of the pulse out of the cavity.

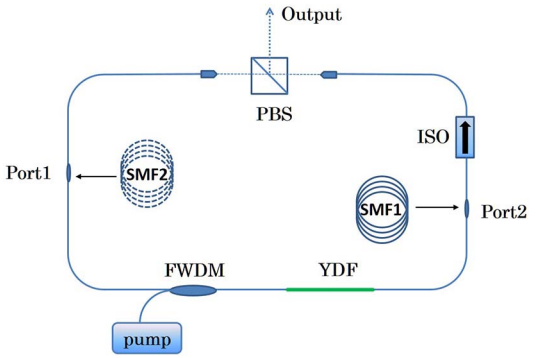

Fig. 1. Setup of the simplified Yb-doped mode-locked fiber laser. Port 1, the extra 20 m SMF (dotted line) located behind the output port; Port 2, the extra 20 m SMF (solid line) located before the output port.

In order to study the nonlinear dynamics in the oscillator, the extra 20 m long SMF is inserted in two different positions, as shown in Fig. 1.

First, we placed an extra SMF (~20 m) behind the output (dotted line), as illustrated in Fig. 1. The self-started mode locking was realized when the pump power exceeded the pump threshold (156 mW). Furthermore, we properly fixed the fiber on the optical bench, and self-started stable mode locking can always be obtained when pump power exceeds the threshold. The pulse shape and pulse train (the insert) under the pump power of 210 mW are shown in Fig. 2(a), and the spectra under different pump powers is showen in Fig. 2(b). Figure 2(a) shows the pulse shape measured by a photodiode and an oscilloscope (MDO3102, Tektronix). The pulse width is 820 ps (FWHM). Figure 2(b) shows the spectra of the mode-locked pulses measured by a spectrometer (AQ6370 C, YOKOGAWA). In this experiment, by fixing the cavity parameter to invariable and then increasing the pump power, the spectrum broadens gradually and the central wavelength locates at 1035–1036 nm, as illustrated in Fig. 2(b). The pulse train stays stable when the pump power gradually increases, and a bit of Raman spectrum occurs when the pump power is 480 mW.

Owing to the laser operated in the ANDi regime, the continuous pulse train formation should balance the cavity dispersion, fiber nonlinearity, gain, and loss. Different from the anomalous dispersion regime, where the pulse shaping is mainly due to the "self-balance" ability between the anomalous dispersion and fiber nonlinearity, in the ANDi regime, a bandwidth limited component is crucial for mode locking. There were no physical bandpass filters or polarization controllers in the oscillator, but mode locking is still obtained. The mechanism of the FBFE[10] can explain the intrinsic mode locking in this oscillator. The cavity birefringence is equivalent to the effective cavity transmission bandwidth. Although the YDF has a broad gain bandwidth, due to the bandpass limitation of the FBFE, the effective gain of the laser has a narrow bandwidth. We demonstrated a more simplified model utilizing

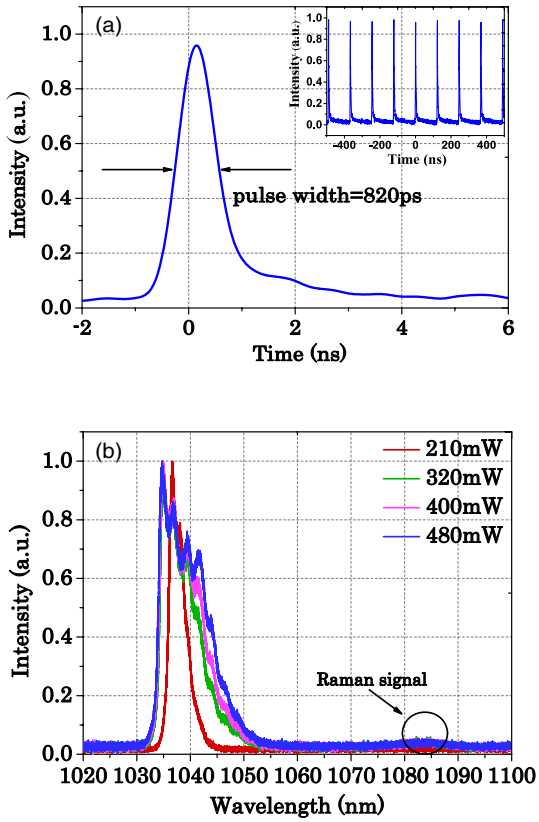

Fig. 2. (Color online) Characteristics of mode-locked operation. (a) The pulse shape and the pulse train (the insert) at pump power of 210 mW, and (b) the spectra under different pump powers.

FBFE for mode locking without the physical filter and polarization controller in the oscillator. Moreover, Fig. 2(b) shows that the filter effect is stronger in the long wavelength than in the short wavelength, and the experiment results are consistent with the numerous simulations[10]. The length of active fiber used in the experiment is 23 cm, which is proper for absorbing pump power effectively, while the gain fiber does not have enough Yb^{3+} to reabsorb the laser photons in the cavity, so the reabsorption effect is negligible. Overall, the FBFE is the main reason for mode locking in the laser setup.

The FBFE acts as a spectral filter in a simplified mode-locked fiber laser, and a DS was achieved[12,28]. The cavity design is applicable for the laser operating in the DS regime. The extra SMFs is long enough to accumulate the nonlinear phase delay for mode locking and obtain a large dispersion to avoid a pulse split. The placing of extra SMF behind the output is important for the pulse type, owing to the nonlinearity accumulation that is not larger than the critical saturation power (CSP) of the FBFE. If the peak power passes over the CSP, the oversaturation of the FBFE can give rise to high modal fluctuations and instabilities, thereby possibly leading to the formation of NLPs[10,19,28,29].

Secondly, we changed the position of the extra SMF and put it before the output as port 2 (solid line), as illustrated

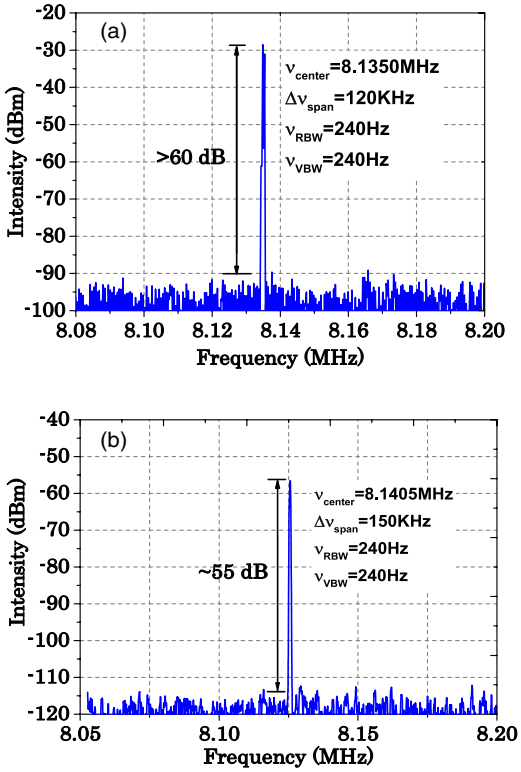

Fig. 3. RF spectrum of the different mode-locked operations. (a) The SMF2 spliced in the cavity, and (b) the SMF1 spliced in the cavity.

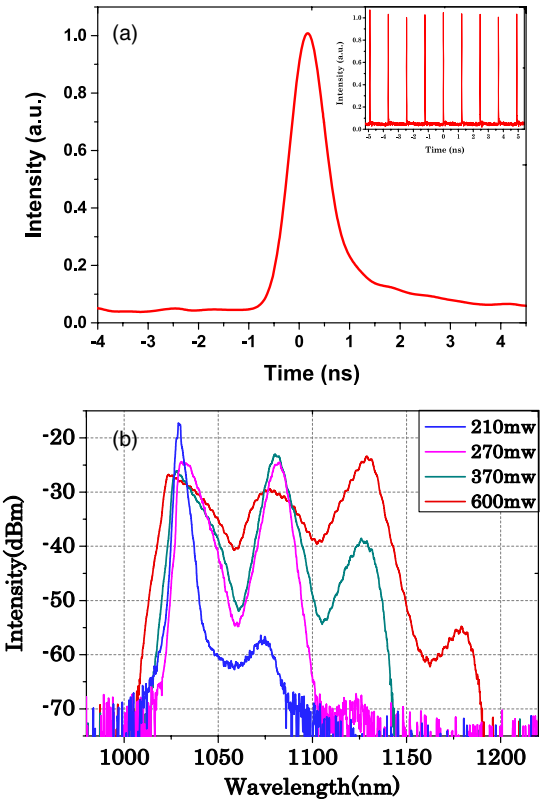

Fig. 4. (Color online) Characteristics of mode-locked operation. (a) Temporal pulse shape is measured at the pump of 370 mW and (b) spectra under different pump powers.

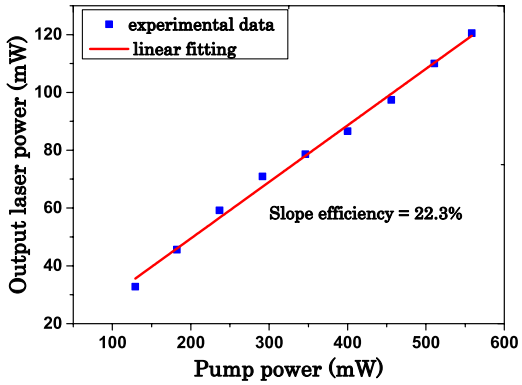

Fig. 5. Average output power versus the incident pump power.

in Fig. 1. The self-started stable mode-locked pulse train was still achieved. The cavity length remains nearly unchanged except fusion loss. From Figs. 3(a) and 3(b), we can speculate that the fiber fusion loss is about 30 mm. The pulse width was measured by the oscilloscope under different pump powers, and the pulse widths that increased with the pump power are shown in Fig. 4(a). Figure 3(a) shows the radio frequency (RF) spectrum with a high contrast of 55 dB. Figure 4(b) shows the evolution of the spectrum when the pump power increases, and the spectra evolution is distinctly different from the spectra evolution in Fig. 2(b). In Fig. 4(b), when the pump power is 210 mW, the central wavelength is 1030 nm, and the corresponding first-order Raman scattering Stokes wave generates and locates at 1075 nm. When the pump power is 270 mW, the first-order Stokes wave is obviously enhanced. When the pump power is 370 mW, the first and second-order Raman scattering Stokes waves generate and locate at 1080 and 1126 nm, respectively. When the pump power is 600 mW, the Raman continuum is generated with cascaded multi-order Stokes waves, and the spectrum extends to 1188 nm. Figure 5 shows the average output power versus the incident pump power, where the pulse forming threshold is 134 mW, and the slope efficiency is 22.3%, indicating that the laser has been optimized for optical-to-optical conversion efficiency.

The evolution of spectra with different pump powers shows that the broader and smoother spectra are generated in the higher pump power. The evolution is closely relative to Raman scattering and the Kerr effect in the fiber oscillator. The result indicates that the laser may operate in the NLP regime[19,28], and the enhanced Raman scattering may collapse the DSs into NLPs[10]. Considering the laser setup, the place of the extra SMF is the only changeable parameter for our contrast experiments, so the FBFE changes a little. It is noteworthy that although the nonlinear phase delay is an influence factor of the FBFE, and the nonlinear accumulation in the oscillator is far above the disturbance of the FBFE, the place of the extra SMF in the oscillator is the main reason for the different results. For instance, once the peak power

eventually reaches the CSP, any further increment in the pulse peak power confirms that the strong gain observed at the Stokes wavelength of the spectrum is due to the SRS progress. New frequency components generated and thereby disrupted the DS pulse formation in the cavity and finally triggered the NLP formation.

In conclusion, we experimentally demonstrate a simple compact fiber laser mode-locked by the FBFE in the ANDi regime based on the NPR technique and give a reason for the nonlinear dynamics of the DS operation and the NLP operation, corresponding the extra SMF location in the cavity. The intra-cavity enhanced SRS progress is a thought for special wavelength generation. The next work is ongoing for an amplifier based on the broadband spectrum oscillator.

This work was supported by the National Natural Science Foundation of China (No. 61575011) and the Key Project of the National Natural Science Foundation of China (No. 61235010).

References

1. C. Xu and F. W. Wise, Nat. Photon. **7**, 875 (2013).
2. A. Chong, J. Buckley, W. Renninger, and F. Wise, Opt. Express **14**, 10095 (2006).
3. H. Ahmad, M. A. M. Salim, Z. A. Ali, M. F. Ismail, and K. Thambiratnam, Chin. Opt. Lett. **13**, 091403 (2015).
4. D. J. Richardson, J. Nilsson, and W. A. Clarkson, J. Opt. Soc. Am. B. **27**, B63 (2010).
5. C. Chédot, C. Lecaplain, S. Idlahcen, G. Martel, and A. Hideur, Fiber Integr. Opt. **27**, 341 (2008).
6. J. Mei, X. Xiao, and C. Yang, Chin. Opt. Lett. **13**, 091403 (2015).
7. W. H. Renninger, A. Chong, and F. W. Wise, Opt. Lett. **33**, 3025 (2008).
8. H. Zhao, L. Chai, C. M. Ouyang, M. L. Hu, and Q. M. Wang, Chin. J. Lasers **12**, 003 (2010).
9. L. J. Kong, X. S. Xiao, and C. X. Yang, Chin. Phys. B **19**, 074212 (2010).
10. L. M. Zhao, D. Y. Tang, X. Wu, and H. Zhang, Opt. Lett. **35**, 2756 (2010).
11. K. Sumimura, H. Yoshida, H. Okada, H. Fujita, and M. Nakatsuka, in *CLEO/Pacific Rim.26* (2007), paper ThP_010.
12. D. J. Li, D. Y. Shen, L. Li, H. Chen, D. Y. Tang, and L. M. Zhao, Appl. Opt. **54**, 7912 (2015).
13. M. Suzuki, R. A. Gannv, S. Yonega, and H. Kuraoda, Opt. Lett. **40**, 804 (2015).
14. C. S. Wang, Phys. Rev. **182**, 482 (1969).
15. P. L. Hsiung, Y. Chen, T. H. Ko, J. G. Fujimoto, S. V. Popov, J. R. Taylor, and V. P. Gapontsev, Opt. Express **12**, 5287 (2004).
16. H. Lim, Y. Jiang, Y. M. Wang, Y. C. Huang, Z. P. Chen, and F. W. Wise, Opt. Lett. **30**, 1171 (2005).
17. M. E. Fermann and I. Hartl, Nat. Photon. **7**, 868 (2013).
18. J. Santhanam and G. P. Agrawal, Opt. Commun. **222**, 413 (2003).
19. T. North and M. Rochette, Opt. Lett. **38**, 890 (2013).
20. K. Yin, B. Zhang, W. Q. Yang, H. W. Chen, and J. Hou, Opt. Express **21**, 15987 (2013).
21. C. Aguergaray, A. Runge, M. Erkintalo, and N. G. R. Broderick, Opt. Lett. **38**, 2644 (2013).
22. A. E. Bednyakova, S. A. Babin, D. S. Kharenko, E. V. Podivilov, M. P. Fedoruk, V. L. Kalashnikov, and A. Apolonski, Opt. Express **21**, 20556 (2013).
23. H. L. Yu, X. J. Xu, X. L. Wang, J. B. Chen, and P. Zhou, Appl. Phys. B **117**, 305 (2014).
24. J. M. Dudley, G. Genty, and S. Coen, Rev. Mod. Phys. **78**, 1135 (2006).
25. A. Chamorovskiy, A. Rantamäki, A. Sirbu, A. Mereuta, E. Kapon, and O. G. Okhotnikov, Opt. Express **18**, 23872 (2010).
26. M. S. Liao, X. Yan, W. Q. Gao, Z. C. Duan, G. S. Qin, T. Suzuki, and Y. Ohishi, Opt. Express **19**, 15389 (2011).
27. H. Sayinc, K. Hausmann, J. Neumann, and D. Kracht, Opt. Express **19**, 25918 (2011).
28. J. Yoonchan, A. V. Luis, L. Seungjong, and K. Youngchul, Opt. Fiber Technol. **20**, 575 (2014).
29. S. Liu, F. P. Yan, Y. Li, L. N. Zhang, and Z. Y. Bai, Photon. Res. **4**, 318 (2016).